New Coupling Schemes for Distribution Broadband over Power Lines (BPL) Networks

Athanasios G. Lazaropoulos*

Abstract—This paper considers the broadband performance of distribution broadband over power lines (BPL) networks when a new refined theoretical coupling scheme computation module (CS2 module) is applied. The broadband performance of distribution BPL networks is investigated in terms of their channel attenuation and capacity in the 3–88 MHz frequency range, which is the typical operating frequency band of BPL technology. The analysis and relevant numerical results outline the important attenuation and capacity improvement of distribution BPL networks when CS2 module is applied.

1. INTRODUCTION

Similar to its original design, today's power grid can become a suitable communications platform either for providing broadband last mile access or for developing an advanced IP-based network with a myriad of smart grid applications when broadband over power lines (BPL) technology features are applied across it [1–9].

To examine the spectral behavior of distribution BPL networks — i.e., overhead and underground medium-voltage (MV) and low-voltage (LV) BPL networks —, the hybrid model is also adopted in this this paper. Extensively employed to examine the behavior of various multiconductor transmission line (MTL) configurations in BPL networks [1–8, 10–16], the hybrid model is modular and consists of: (i) a bottom-up approach that is based on an appropriate combination of MTL theory and similarity transformations; and (ii) a top-down approach that is based on the concatenation of multidimensional transmission matrices of the cascaded network BPL connections. During the top-down approach, a coupling scheme computation module defines the way that BPL signals are injected onto and extracted from the power lines of distribution BPL connections. Then, based on the hybrid model, several useful broadband performance metrics such as channel attenuation and capacity of the distribution BPL networks can be assessed when different coupling schemes are applied [2–7, 10, 17–19].

In this paper, a theoretical coupling scheme computation module (CS2 module) that defines a more general and efficient version of the existing simple CS1 module is proposed. Actually, in comparison with CS1 module, CS2 module better exploits: (i) all the available conductors of the MTL configurations so as to propose state-of-the-art coupling schemes with conductor participation percentage; and (ii) the injected and extracted power of signals at the transmitting and receiving ends of BPL connections. Therefore, CS2 module achieves better broadband performance metrics compared to the existing ones since it exceeds the today's limitations of CS1 module through the use of the proposed BPL signal coupling procedure of two interfaces.

The rest of this paper is organized as follows. In Section 2, the overhead and underground MV and LV MTL configurations as well as the respective indicative BPL topologies are demonstrated. On the basis of the hybrid model, Section 3 synopsizes the basics of BPL signal propagation and transmission. Special attention is given to the role of coupling schemes and, especially, to CS2 module and its BPL

signal coupling procedure. Section 4 deals with electromagnetic interference (EMI) issues, noise and capacity of distribution BPL networks. In Section 5, numerical results and discussion are provided, aiming at revealing the refreshing role of CS2 module; say, better channel attenuation and capacity performance in comparison with the existing CS1 module. Section 6 concludes this paper.

2. DISTRIBUTION POWER GRIDS

2.1. Overhead MV and LV MTL Configuration

A typical case of an overhead MV distribution line is depicted in Fig. 1(a). Overhead MV distribution lines hang at typical heights h^{OVMV} above ground. These overhead MV lines consist of three parallel non-insulated phase conductors spaced by Δ^{OVMV}. This three-phase three-conductor ($n^{OVMV} = 3$) overhead MV distribution line configuration is considered in the present work consisting of steel reinforced aluminum conductors (ACSR conductors) [1, 3, 4, 12, 20, 21].

The overhead LV distribution line that will be examined in this paper is depicted in Fig. 1(b). Four parallel non-insulated conductors are suspended one above the other spaced by Δ^{OVLV} and located at
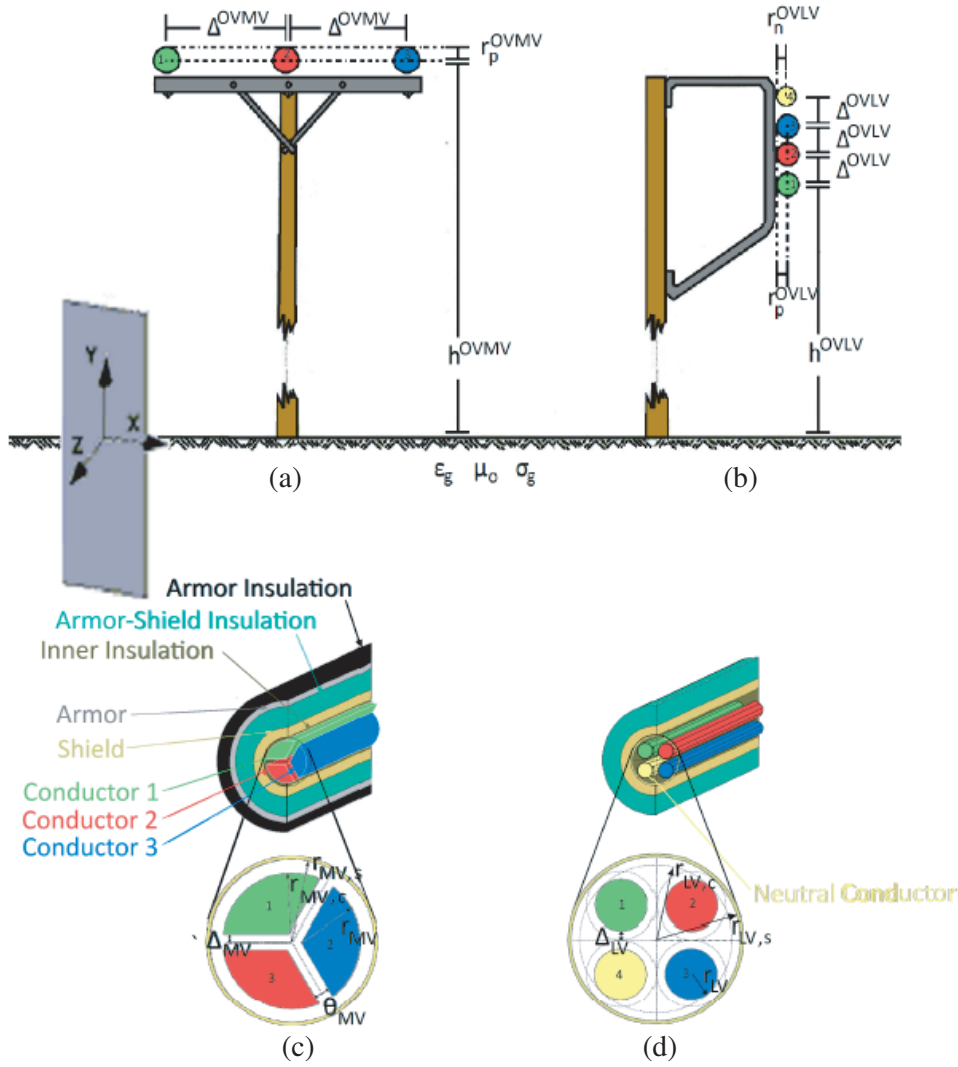
Figure 1. Typical MTL configurations. (a) Overhead MV [1]. (b) Overhead LV [1]. (c) Underground MV [1]. (d) Underground LV [2].

heights h^{OVLV} above ground for the lowest conductor. The upper conductor is the neutral, while the lower three conductors are the three phases. This three-phase four-conductor ($n^{\text{OVLV}} = 4$) overhead LV distribution line configuration consists of ACSR conductors [1].

2.2. Underground MV and LV MTL Configuration

The UN MV distribution line that will be examined is the three-phase sector-type Paper Insulated Lead Covered (PILC) distribution-class cable depicted in Fig. 1(c). This cable arrangement consists of the three-phase three-sector-type conductors ($n^{\text{UNMV}} = 3$), one shield conductor and one armor conductor while the shield and the armor are grounded at both ends [1, 5, 22–24].

The UN LV distribution line that will be examined is the three-phase four-conductor ($n^{\text{UNLV}} = 4$) core-type distribution cable depicted in Fig. 1(d). This cable arrangement consists of the three-phase three-core-type conductors, one core-type neutral conductor and one shield conductor. Since there is no armor in this UN LV distribution line, only the shield is grounded at both ends [2, 13, 14, 21, 25, 26].

2.3. Ground and Reference Conductors

In all the cases examined, the conductivity of the ground is assumed $\sigma_{\text{g}} = 5\,\text{mS/m}$ and its relative permittivity $\varepsilon_{\text{rg}} = 13$, which define a realistic scenario [1, 3, 4, 7, 10–12].

As it concerns the overhead distribution MTL configurations, the impact of imperfect ground on signal propagation via overhead distribution power lines was analyzed in [2–7, 10–12, 20, 27–29]. Here, the ground is considered as the reference conductor.

As it concerns the underground distribution MTL configurations, the analytical formulation, which is adopted in this paper, considers high frequency propagation in the general case of underground power lines consisting of multiple conductors within common shield and analysed in [2, 5–7, 13, 14, 25, 30]. Here, the grounded shield is considered as the reference conductor.

2.4. Indicative Distribution BPL Topologies

To compensate the significant distance- and frequency-dependent attenuation of BPL signals, BPL networks are modified through the insertion of repeaters where a repeater is a device that boosts the distance the BPL signal can propagate. Hence, BPL networks are divided into cascaded BPL connections that are bounded by repeaters.

To apply the hybrid model, the simple BPL connection of Fig. 2(a) is considered. This simple BPL connection is bounded by the transmitting end (repeater A) and receiving end (repeater B) while having N branches. Since the number of branches differs depending on the examined connection, each BPL connection is characterized by its BPL topology. To cope with different BPL topologies, the simple BPL connection is assumed to be separated into segments (network modules) that comprise the successive branches encountered — see Figs. 2(a) and 2(b) —. With reference to Fig. 2(c), the cascade of network modules corresponds to the topology of the BPL connection.

With reference to [1] and Fig. 2(a), average path lengths $L = L_1 + \ldots + L_{N+1}$ of the order of 1000 m and 200 m are considered for overhead distribution — i.e., overhead MV and LV- and for underground distribution — i.e., underground MV and LV-BPL connections, respectively.

As it concerns the overhead distribution BPL connections, five indicative overhead distribution BPL topologies of average path length, which are common for both overhead MV and overhead LV BPL connections, are examined. Their topological characteristics are detailed in Table 1. Similarly to overhead distribution BPL connections, five indicative underground distribution BPL topologies of average path length are examined in this paper. As in the overhead distribution BPL case, the underground distribution BPL topologies are common for both underground MV and underground LV BPL connections and are detailed in Table 2.

The circuital parameters of the above indicative distribution BPL topologies are reported in [1–8, 10, 12, 14, 21, 22, 31–33]. Analytically, the cables of the branching lines are assumed identical to the distribution ones while the interconnections between the distribution and branch lines are assumed to be fully activated. The transmitting and the receiving ends are assumed matched to the characteristic impedance of the distribution lines whereas the branch terminations are assumed open circuit.
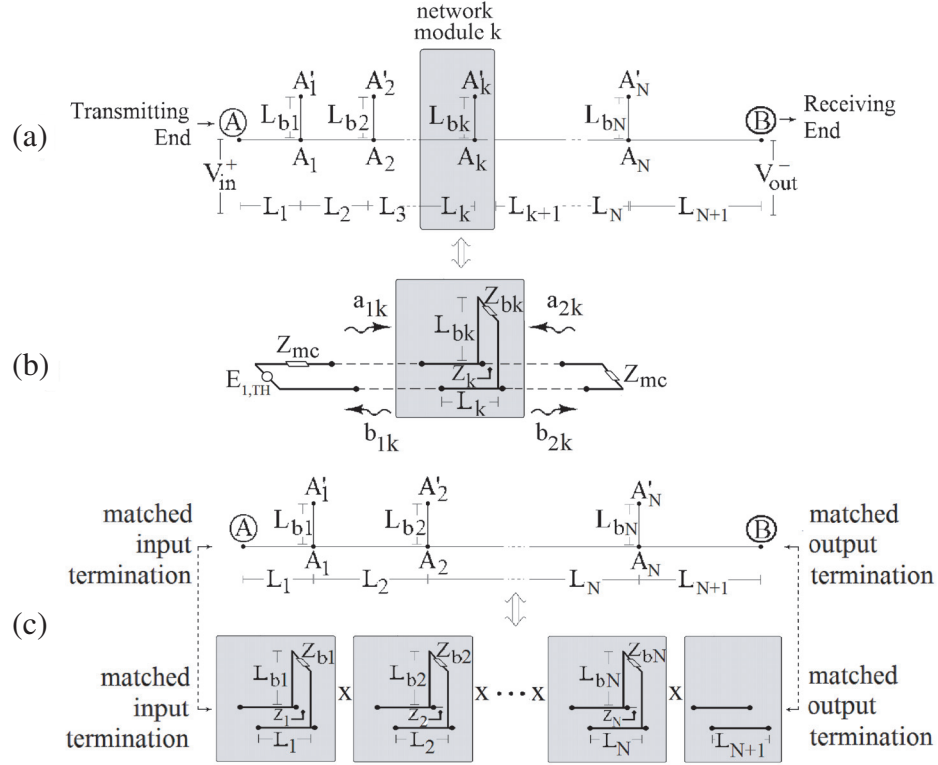
Figure 2. (a) End-to-end BPL connection with N branches. (b) Network module. (c) An indicative BPL topology considered as a cascade of $N+1$ modules corresponding to N branches [1].

Table 1. Overhead distribution BPL topologies.

Topology Name	Topology Description	Number of Branches	Length of Distribution Lines	Length of Branching Lines
Urban case A	Typical overhead urban topology	3	$L_1 = 500\,\mathrm{m}$, $L_2 = 200\,\mathrm{m}$, $L_3 = 100\,\mathrm{m}$, $L_4 = 200\,\mathrm{m}$	$L_{b1} = 8\,\mathrm{m}$, $L_{b2} = 13\,\mathrm{m}$, $L_{b3} = 10\,\mathrm{m}$
Urban case B	Aggravated overhead urban topology	5	$L_1 = 200\,\mathrm{m}$, $L_2 = 50\,\mathrm{m}$, $L_3 = 100\,\mathrm{m}$, $L_4 = 200\,\mathrm{m}$, $L_5 = 300\,\mathrm{m}$, $L_6 = 150\,\mathrm{m}$	$L_{b1} = 12\,\mathrm{m}$, $L_{b2} = 5\,\mathrm{m}$, $L_{b3} = 28\,\mathrm{m}$, $L_{b4} = 41\,\mathrm{m}$, $L_{b5} = 17\,\mathrm{m}$
Suburban case	Overhead suburban topology	2	$L_1 = 500\,\mathrm{m}$, $L_2 = 400\,\mathrm{m}$, $L_3 = 100\,\mathrm{m}$	$L_{b1} = 50\,\mathrm{m}$, $L_{b2} = 10\,\mathrm{m}$
Rural case	Overhead rural topology	1	$L_1 = 600\,\mathrm{m}$, $L_2 = 400\,\mathrm{m}$	$L_{b1} = 300\,\mathrm{m}$
"LOS" case	Overhead Line-of-Sight transmission	0	$L_1 = 1000\,\mathrm{m}$	-

3. THE PRINCIPLES OF BPL SIGNAL PROPAGATION, TRANSMISSION AND COUPLING — THE HYBRID MODEL

3.1. Bottom-Up Approach

The first key element of the hybrid model is its bottom-up approach that deals with the signal propagation across MTL configurations of distribution BPL networks. As it has already been

Table 2. Underground distribution BPL topologies.

Topology Name	Topology Description	Number of Branches	Length of Distribution Lines	Length of Branching Lines
Urban case A	Typical underground urban topology	3	$L_1 = 70\,\text{m}$, $L_2 = 55\,\text{m}$, $L_3 = 45\,\text{m}$, $L_4 = 30\,\text{m}$	$L_{b1} = 12\,\text{m}$, $L_{b2} = 7\,\text{m}$, $L_{b3} = 21\,\text{m}$
Urban case B	Aggravated underground urban topology	5	$L_1 = 40\,\text{m}$, $L_2 = 10\,\text{m}$, $L_3 = 20\,\text{m}$, $L_4 = 40\,\text{m}$, $L_5 = 60\,\text{m}$, $L_6 = 30\,\text{m}$	$L_{b1} = 22\,\text{m}$, $L_{b2} = 12\,\text{m}$, $L_{b3} = 8\,\text{m}$, $L_{b4} = 2\,\text{m}$, $L_{b5} = 17\,\text{m}$
Suburban case	Underground suburban topology	2	$L_1 = 50\,\text{m}$, $L_2 = 100\,\text{m}$, $L_3 = 50\,\text{m}$	$L_{b1} = 60\,\text{m}$, $L_{b2} = 30\,\text{m}$
Rural case	Underground rural topology	1	$L_1 = 50\,\text{m}$, $L_2 = 150\,\text{m}$	$L_{b1} = 100\,\text{m}$
"LOS" case	Underground Line-of-Sight transmission	0	$L_1 = 200\,\text{m}$	-

mentioned in [1–7, 10, 11, 15], through a matrix approach, bottom-up approach can extend the standard transmission line (TL) analysis to the MTL one, which involves more than two conductors. Similarly to a two-conductor line where one forward- and one backward-traveling wave are supported, a MTL structure with $n^{\text{G}} + 1$ conductors may support n^{G} pairs of forward- and backward-traveling waves with corresponding propagation constants where $[\cdot]^{\text{G}}$ denotes the examined power grid type — either overhead MV or underground MV or overhead LV or underground LV — Each pair of forward- and backward-traveling waves is referred to as a mode. Each of the n^{G} modes propagates across BPL connections while their spectral behavior has thoroughly investigated in [1–7, 10–15, 20, 21, 26–29].

3.2. Top-Down Approach

The second key element of the hybrid model is its top-down approach (i.e., TM2 method) that describes the signal transmission across the BPL connections. TM2 method is based on the concatenation of multidimensional transmission matrices of the cascaded network BPL connections and presented analytically in [1]. In accordance with [1], the spectral behavior of the supported modes by each MTL configuration is described through the $n^{\text{G}} \times n^{\text{G}}$ eigenvalue decomposition (EVD) modal transfer function matrix $\mathbf{H}^{\text{m}}\{\cdot\}$ whose elements $H_{i,j}^{\text{m}}\{\cdot\}$, $i, j = 1, \ldots, n^{\text{G}}$ are the EVD modal transfer functions where $H_{i,j}^{\text{m}}$ denotes the element of the matrix $\mathbf{H}^{\text{m}}\{\cdot\}$ in the row i of the column j.

With reference to Figs. 3(a) and 3(b), the $n^{\text{G}} \times n^{\text{G}}$ channel transfer function matrix $\mathbf{H}^{\text{m}}\{\cdot\}$ that relates line voltages $\mathbf{V}(z) = [V_1(z) \ \cdots \ V_{n^{\text{G}}}(z)]^{\text{T}}$ at the transmitting ($z = 0$) and the receiving ($z = L$) ends is determined from

$$\mathbf{H}\{\cdot\} = \mathbf{T}_{\text{V}} \cdot \mathbf{H}^{\text{m}}\{\cdot\} \cdot \mathbf{T}_{\text{V}}^{-1} \tag{1}$$

where $[\cdot]^{\text{T}}$ denotes the transpose of a matrix, and $\mathbf{T}_{\text{V}}$ is a $n^{\text{G}} \times n^{\text{G}}$ matrix depending on the frequency, power grid type, physical properties of the cables and geometry of the MTL configuration.

3.3. CS2 Module, Its BPL Signal Coupling Procedure and Its Supported Coupling Schemes

According to how signals are injected onto and extracted from the lines of a MTL configuration, different coupling schemes may exist [1, 4, 7, 10–12]. With reference to Figs. 3(a) and 3(b), CS2 module describes the BPL signal coupling procedure using two interfaces, namely:

(1) *BPL signal injection interface*: It is located at the transmitting end — see Fig. 3(a) —. Through the input coupling $n^{\text{G}} \times 1$ column vector $\mathbf{C}^{\text{in}}$, this interface relates the line voltages
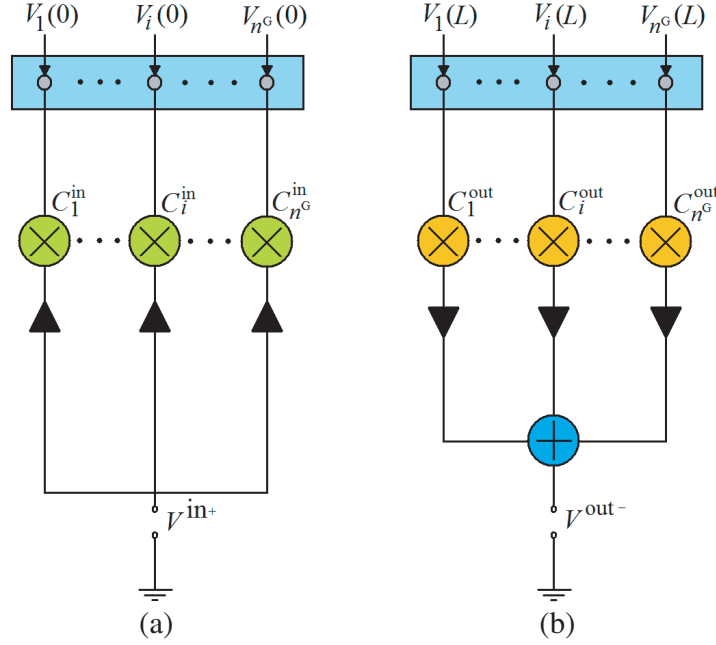
Figure 3. CS2 module. (a) BPL signal injection interface at the transmitting end. (b) BPL signal extraction interface at the receiving end.

$\mathbf{V}(0) = [V_1(0) \ \ldots \ V_{n^{\mathrm{G}}}(0)]^{\mathrm{T}}$ with the input BPL signal $V^{\mathrm{in}+}$ through

$$\mathbf{V}(0) = V^{\mathrm{in}+} \cdot \mathbf{C}^{\mathrm{in}} \tag{2}$$

The input BPL signal $V^{\mathrm{in}+}$ carries all the required information that needs to be transmitted through the BPL connection. The elements C_i^{in}, $i = 1, \ldots, n^{\mathrm{G}}$ of the input coupling vector $\mathbf{C}^{\mathrm{in}}$ are the input coupling coefficients as well as the participation percentages of the conductors of the MTL configurations during the BPL signal injection; the sum of their absolute values is equal to one while their signs indicate the propagation direction of BPL signal.

(2) *BPL signal extraction interface*: It is located at the receiving end — see Fig. 3(b) — and, through its output coupling $1 \times n^{\mathrm{G}}$ line vector $\mathbf{C}^{\mathrm{out}} = [C_1^{out} \ \ldots \ C_{n^{\mathrm{G}}}^{out}]^{\mathrm{T}}$, it relates the output BPL signal $V^{\mathrm{out\text{-}}}$ with the line voltages $\mathbf{V}(L) = [V_1(L) \ \ldots \ V_{n^{\mathrm{G}}}(L)]^{\mathrm{T}}$ through

$$V^{out-} = \mathbf{C}^{\mathrm{out}} \cdot \mathbf{V}(L) \tag{3}$$

where C_i^{out}, $i = 1, \ldots, n^{\mathrm{G}}$ are the extraction coefficients. Note that the output BPL signal V^{out-} delivers at the receiving end the information that has been transmitted at the transmitting end.

Taking under consideration that: (i) during BPL signal coupling, there is neither amplification nor attenuation of BPL signal; (ii) the sum of the absolute values of participation percentages at the transmitting end is equal to one due to the conservation of energy; and (iii) in order to optimize the reception of BPL signal, the output BPL signal V^{out-} must be equal to the input BPL signal V^{in+} when the BPL channel attenuation is neglected — i.e., $\mathbf{C}^{\mathrm{in}}$ and $\mathbf{C}^{\mathrm{out}}$ must be orthonormal matrices —; the following three equations need to be simultaneously satisfied:

$$\left|C_i^{\mathrm{in}}\right| \leq 1, \ \left|C_i^{\mathrm{out}}\right| \leq 1, \ i = 1, \ldots, n^{\mathrm{G}} \tag{4}$$

$$\sum_{i=1}^{n^{\mathrm{G}}} \left|C_i^{\mathrm{in}}\right| = 1 \tag{5}$$

$$\sum_{i=1}^{n^{\mathrm{G}}} C_i^{\mathrm{out}} \cdot C_i^{\mathrm{in}} = 1 \tag{6}$$

By definition, CS2 module is a lossy transformation since it is based on the usual discrete-orthogonal-wavelet transform. However, by adopting the CS2 module, a signal adapted orthogonal basis is used taking advantage of its voltage-branch architecture. The final decomposition, being orthonormal see Eq. (6), will conserve the energy as expected.

Based on: (i) the presented BPL signal coupling procedure of CS2 module; (ii) the $n^{\mathrm{G}} \times n^{\mathrm{G}}$ channel transfer function matrix $\mathbf{H}\{\cdot\}$ of Eq. (1); (iii) the relation between line quantities and input/output ones as determined from Eqs. (2) and (3); and (iv) the restrictions of Eqs. (4)–(6); the CS2 module proposes the coupling scheme channel transfer function that relates output and input BPL signal through

$$H^{\mathrm{C}}\{\cdot\} = \frac{[V^{\mathrm{out\text{-}}}]^{\mathrm{C}}}{[V^{\mathrm{in+}}]^{\mathrm{C}}} = [\mathbf{C}^{\mathrm{out}}]^{\mathrm{C}} \cdot \mathbf{H}\{\cdot\} \cdot [\mathbf{C}^{\mathrm{in}}]^{\mathrm{C}} \tag{7}$$

where $[\cdot]^{\mathrm{C}}$ denotes the applied coupling scheme. On the basis of Eq. (7) and depending on the form of $\mathbf{C}^{\mathrm{in}}$ and $\mathbf{C}^{\mathrm{out}}$, CS2 module can support three types of coupling schemes, namely:

(1) *Coupling Scheme Type 1: Wire-to-Ground (WtG) or Shield-to-Phase (StP) coupling schemes.* The signal is injected into only one conductor at the transmitting end and returns via the ground or the shield for overhead or underground BPL connections, respectively. The signal is extracted from the same conductor at the receiving end.

  Hereafter, WtG or StP coupling between conductor s, $s = 1, \ldots, n^{\mathrm{G}}$ and ground or shield will be detoned as WtG^s or StP^s, respectively.

  Based on Eqs. (2), (3), and (4)–(6), $[\mathbf{C}^{\mathrm{in}}]^{\mathrm{WtG}^s/\mathrm{StP}^s}$ and $[\mathbf{C}^{\mathrm{out}}]^{\mathrm{WtG}^s/\mathrm{StP}^s}$ have zero elements except in line s and row s, respectively, where the value is equal to 1. This type of coupling scheme remains the same in comparison with the vintage CS1 module of [1, 4, 7, 10–12].

(2) *Coupling Scheme Type 2: Wire-to-Wire (WtW) or Phase-to-Phase (PtP) coupling schemes.* The signal is injected in equal parts between two conductors. The signal is extracted from the same conductors.

  WtW or PtP coupling between conductors p and q, $p.q = 1, \ldots, n^{\mathrm{G}}$ will be detoned as WtW^{p-q} or PtP^{p-q}, respectively.

  Based on Eqs. (2), (3), and (4)–(6), $[\mathbf{C}^{\mathrm{in}}]^{\mathrm{WtW}^{p-q}/\mathrm{PtP}^{p-q}}$ has zero elements except in lines p and q where the values are equal to 0.5 and -0.5, respectively, whereas, $[\mathbf{C}^{\mathrm{out}}]^{\mathrm{WtW}^{p-q}/\mathrm{PtP}^{p-q}}$ has zero elements except in rows p and q where the values are equal to 1 and -1, respectively.

  Note that this type of coupling schemes have also been employed in the CS1 module with, however, different values concerning the BPL signal extraction interface are used [1, 4, 7, 10–12]; say, $[\mathbf{C}^{\mathrm{out}}]^{\mathrm{WtW}^{p-q}/\mathrm{PtP}^{p-q}}$ has zero elements except in rows p and q where the values are equal to 0.5 and -0.5. As it is going to be validated and analyzed in Section 5, this value selection significantly degrades the broadband performance of WtW or PtP coupling schemes.

(3) *Coupling Scheme Type 3: MultiWire-to-MultiWire (MtM) or MultiPhase-to-MultiPhase (MtM) coupling schemes.* The signal is injected among multiple conductors with different participation percentages for overhead or underground BPL connections, respectively. Similarly to the previous coupling scheme types, the signal is extracted from the same conductor set at the receiving end.

  As the MtM coupling scheme notation is concerned, for example, MtM coupling scheme among the three conductors p, q and r, $p, q, r = 1, \ldots, n^{\mathrm{G}}$ with participation percentages equal to C_p^{in}, C_q^{in} and C_r^{in}, respectively, will be detoned as $\mathrm{MtM}^{p-q-r}_{C_p^{\mathrm{in}}-C_q^{\mathrm{in}}-C_r^{\mathrm{in}}}$. Based on Eqs. (2), (3) and (4)–(6), at the transmitting end, $[\mathbf{C}^{\mathrm{in}}]^{\mathrm{MtM}^{p-q-r}_{C_p^{\mathrm{in}}-C_q^{\mathrm{in}}-C_r^{\mathrm{in}}}}$ has zero elements except in lines p, q and r where the values are equal to C_p^{in}, C_q^{in} and C_r^{in}, respectively, whereas, at the receiving end, $[\mathbf{C}^{\mathrm{out}}]^{\mathrm{MtM}^{p-q-r}_{C_p^{\mathrm{in}}-C_q^{\mathrm{in}}-C_r^{\mathrm{in}}}}$ has zero elements except in rows p, q and r where the values are equal to $\frac{|C_p^{\mathrm{in}}|}{C_p^{\mathrm{in}}}$, $\frac{|C_q^{\mathrm{in}}|}{C_q^{\mathrm{in}}}$ and $\frac{|C_r^{\mathrm{in}}|}{C_r^{\mathrm{in}}}$, respectively.

  Note that this coupling scheme type of CS2 module is firstly proposed in this paper, and due to its adaptive nature, it can exploit the strong points of the supported modal channels of MTL configurations but with a cost analyzed in Section 5.3.

4. EMI POLICIES, NOISE AND CAPACITY OF DISTRIBUTION BPL NETWORKS

4.1. EMI Policies and Power Constraints

A great number of regulatory bodies has established proposals (EMI policies) as well as respective injected power spectral density limits (IPSD limits) concerning the BPL operation. By adopting these EMI policies, the emissions from BPL networks are regulated so as not to interfere with the other already existing communications services in the same frequency band of operation.

Regardless of the applied coupling scheme, the injected power spectral density limits (IPSD limits) proposed by Ofcom provide a presumption of compliance with the current FCC Part 15 [1–8, 10, 34–40]. Synoptically, in the 3–30 MHz frequency range, maximum levels of -60 dBm/Hz and -40 dBm/Hz constitute appropriate IPSD limits $p(f)$ for overhead and underground BPL networks, respectively, whereas in the 30–88 MHz frequency range, maximum IPSD limits $p(f)$ equal to -77 dBm/Hz and -57 dBm/Hz for the respective overhead and underground BPL networks are assumed.

4.2. Noise Characteristics

As it concerns the noise properties of BPL networks in the 3–88 MHz frequency range, a uniform additive white Gaussian noise (AWGN) PSD levels $N(f)$ will be assumed equal to -105 dBm/Hz and -135 dBm/Hz in the case of overhead and underground BPL networks, respectively [1–8].

4.3. Capacity

Capacity is defined as the maximum achievable transmission rate that can be reliably transmitted over a BPL connection and depends on the applied MTL configuration, the BPL topology, the coupling scheme applied, the EMI policies adopted and the noise environment [1–8]. The capacity C for given coupling scheme channel is determined from

$$C = f_{\mathrm{s}} \cdot \sum_{q=0}^{Q-1} \log_2 \left\{ 1 + \left[\frac{\langle p\left(q \cdot f_{\mathrm{s}}\right)\rangle_{\mathrm{L}}}{\langle N\left(q \cdot f_{\mathrm{s}}\right)\rangle_{\mathrm{L}}} \cdot \left| H^{\mathrm{C}}\left(q \cdot f_{\mathrm{s}}\right)\right|^2 \right] \right\} \tag{8}$$

where $\langle \cdot \rangle_{\mathrm{L}}$ is an operator that converts dBm/Hz into a linear power ratio (W/Hz), Q the number of subchannels in the BPL signal frequency range of interest and f_{s} the flat-fading subchannel frequency spacing.

5. NUMERICAL RESULTS AND DISCUSSION

The numerical results of various coupling schemes for different power grid types and BPL topologies aim at investigating: (a) the performance improvement that offers the adoption of the CS2 module when the traditional coupling schemes of CS1 module are considered — i.e., coupling scheme type 1 and 2 —; and (b) the performance metrics of the coupling scheme type 3 that is only supported by the CS2 module.

5.1. Coupling Scheme Type 1

The broadband performance, in terms of channel attenuation and capacity in the 3–88 MHz frequency band, is assessed by applying CS2 and CS1 module when the indicative overhead and underground distribution BPL topologies of Section 2.4 are considered. In this subsection, all the available coupling schemes of type 1 are examined so that direct performance comparison between CS2 and CS1 module can be noticed. Also, the broadband performance metrics remain the same when the coupling configurations of the involved conductors are inverted (i.e., StP^2 and PtS^2 coupling schemes present the same attenuation and capacity results).

In Fig. 4(a), the channel attenuation is plotted versus frequency for the indicative overhead MV/BPL topologies when WtG^1 coupling scheme of the traditional CS1 module is applied. In Fig. 4(b), the channel attenuation is plotted versus frequency for the indicative underground MV/BPL topologies
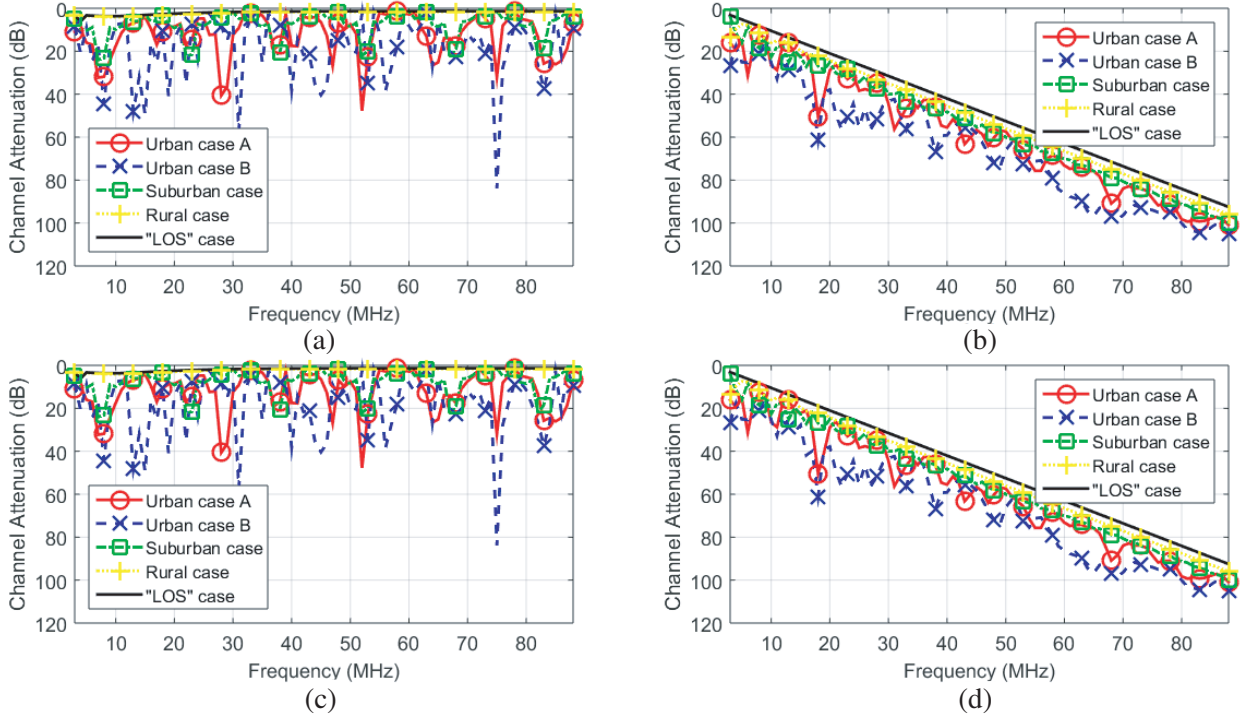
Figure 4. Channel attenuation of indicative topologies in the 3–88 MHz frequency band when coupling schemes of type 1 are applied (the frequency spacing is equal to 1MHz). (a) OV MV/WtG^1 coupling scheme/CS1 module. (b) UN MV/StP^2 coupling scheme/CS1 module. (c) OV MV/WtG^1 coupling scheme/CS2 module. (d) UN MV/StP^2 coupling scheme/CS2 module.

when StP^2 coupling scheme of the CS1 module is applied. In Figs. 4(c) and 4(d), same curves with Figs. 4(a) and 4(b) are given but in the case of the CS2 module.

Observing Figs. 4(a)–(d), it is evident that the channel attenuation remains the same regardless of the applied CS module when random coupling schemes of type 1 are considered. In accordance with Section 3.3, this is an expected outcome since no changes during the mathematical procedure of BPL signal injection and extraction are made within CS2 module.

In fact, the previous coincidence of channel attenuation results is reflected on respective capacity results of Table 3. In Table 3, the capacity of all the indicative distribution BPL topologies of Section 2.4 is reported when all the available coupling schemes of type 1 are applied for the CS1 and CS2 module. Conversely to overhead MTL configurations, it is observed that same capacity results are observed among different StP coupling schemes for given power grid type and BPL topology due to the symmetry of the examined underground MTL configurations.

5.2. Coupling Scheme Type 2

Already mentioned in Section 3.3, CS2 module exploits the orthonormality of the input and output coupling vectors. Hence, CS2 module can achieve better broadband performance due to its improved interface of BPL signal extraction. Although the broadband performance difference between CS1 and CS2 module remains trivial during coupling schemes of type 1, this difference becomes significant in coupling scheme type 2.

Indeed, in Fig. 5(a), the channel attenuation is plotted versus frequency for the indicative overhead LV/BPL topologies when WtW$^{1-3}$ coupling scheme of the traditional CS1 module is applied. In Fig. 5(b), the channel attenuation is plotted versus frequency for the indicative underground LV/BPL topologies when PtP$^{2-4}$ coupling scheme of the CS1 module is applied. In Figs. 5(c) and 5(d), same curves with Figs. 5(a) and 5(b) are given but in the case of the CS2 module.

Table 3. Capacity comparison of CS1 and CS2 module for different coupling schemes of type 1 (CS1 module: blue/CS2 module: red and the frequency spacing is equal to 0.1 MHz).

Power Grid Type	Coupling Schemes	Capacity (Mbps)				
		MV				
		Urban Case A	Urban Case B	Suburban Case	Rural Case	"LOS" case
Overhead	WtG^1	596/596	459/459	705/705	787/787	892/892
	WtG^2	599/599	462/462	709/709	790/790	896/896
	WtG^3	596/596	459/459	705/705	787/787	892/892
	WtG^4	-	-	-	-	-
Underground	StP^1	815/815	685/685	890/890	968/968	1049/1049
	StP^2	815/815	685/685	890/890	968/968	1049/1049
	StP^3	815/815	685/685	890/890	968/968	1049/1049
	StP^4	-	-	-	-	-
		LV				
Overhead	WtG^1	606/606	469/469	715/715	797/797	902/902
	WtG^2	608/608	471/471	717/717	799/799	904/904
	WtG^3	609/609	472/472	719/719	800/800	906/906
	WtG^4	606/606	470/470	716/716	798/798	903/903
Underground	StP^1	1849/1849	1634/1634	1953/1953	2053/2053	2152/2152
	StP^2	1849/1849	1634/1634	1953/1953	2053/2053	2152/2152
	StP^3	1849/1849	1634/1634	1953/1953	2053/2053	2152/2152
	StP^4	1849/1849	1634/1634	1953/1953	2053/2053	2152/2152

From Figs. 5(a)–(d), it is obvious that CS2 module succeeds in reducing channel attenuation by 6 dB in all the cases examined. This improvement is due to the fact that CS1 module only permits the extraction of the one half of the BPL signal at the receiving end whereas the proposed output coupling vector of the CS2 module achieves to restore the entire BPL signal at the receiving end because of its orthonormal elements.

The upgrade of the BPL signal extraction interface that is provided by the CS2 module also improves the respective capacity results of coupling schemes of type 2. In Table 4, the capacity of all the indicative distribution BPL topologies of Sec.IID is reported when all the available coupling schemes of type 2 are applied for the CS1 and CS2 module.

From Figs. 5(a)–(d) and Table 4, several interesting remarks regarding the operation of CS2 module can be deduced:

- The 6 dB channel attenuation gain that is achieved by the BPL signal extraction interface of CS2 module is translated into approximately 160 Mbps capacity gain. In fact, CS2 module renders WtW/PtP coupling schemes almost equivalent to respective WtG/StP ones in terms of channel attenuation and capacity in all the BPL topologies examined.

- Similarly to the coupling schemes of type 1, due to the symmetry of distribution MTL configurations, comparable attenuation and capacity values are observed among different coupling schemes for given power grid type. Also, it should be noted that there is no attenuation and capacity difference in coupling schemes of type 2 if the coupling configurations of the involved conductors are inverted (i.e., WtW$^{1-2}$ and WtW$^{2-1}$ coupling schemes present the same attenuation and capacity results).

- In combination with their favourable characteristics concerning the reduced EMI to the other already existing communications services [12, 20], coupling schemes of type 2 are going to be qualified for the future's BPL network deployment. Actually, the low EMI of coupling schemes of type 2 results from the differential excitation of the conductors, which blocks the propagation of the common mode across the BPL networks [1–7, 12–15, 20, 21, 26–29].
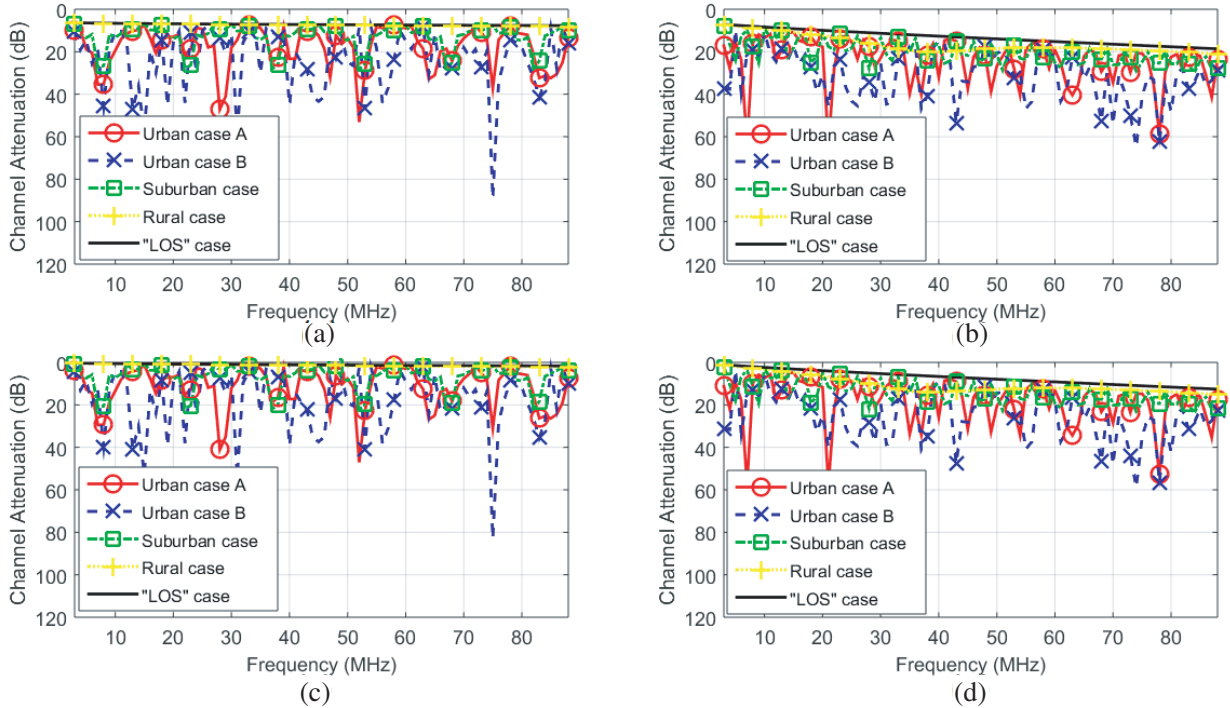
Figure 5. Channel attenuation of indicative topologies in the 3–88 MHz frequency band when coupling schemes of type 2 are applied (the frequency spacing is equal to 1 MHz). (a) OV LV/WtW$^{1-3}$ coupling scheme/CS1 module. (b) UN LV/PtP$^{2-4}$ coupling scheme/CS1 module. (c) OV LV/WtW$^{1-3}$ coupling scheme/CS2 module. (d) UN LV/PtP$^{2-4}$ coupling scheme/CS2 module.

Finally, comparing Tables 3 and 4, it is shown that the same BPL networks present an increase in their capacity by applying the CS2 module. As the examined BPL network remains the same and only the selected input and output ports of the applied coupling schemes are different, the lower channel attenuation of the WtW (PtP) coupling schemes against WtG (StP) ones is reflected on respective higher capacity values.

5.3. Coupling Scheme Type 3

CS2 module allows the introduction of a hybrid coupling scheme type that exploits the strong points of the aforementioned two types. On the basis of the conductor participation percentage, the coupling scheme type 3 offers a plethora of coupling schemes whose broadband performance is highlighted in this subsection.

Already mentioned in Section 3.3 and according to Eq. (4), as it concerns the definition of conductor participation percentage in the input coupling vector, there are two and three participation percentages that can be arbitrarily adjusted from the user for the examined MV and LV MTL configurations, respectively. The last participation percentage is defined in accordance with Eq. (5). Since conductor participation percentages are set in the input coupling vector, the definition of the respective percentages in the output coupling vector is a straightforward procedure following the guidelines of Section 3.3 and Eq. (6).

In general terms, good attenuation results entail promising capacity ones. Hence, only the capacity of the coupling schemes of type 3 is demonstrated in this subsection. Furthermore, only one type of the indicative BPL topologies is further examined (say, LOS case) without affecting the generality of the following analysis.

To assess the performance of MtM coupling schemes, the capacity of the best five MtM ones for each distribution power grid type is presented in Table 5. For each MtM coupling scheme, its participating conductors, the participation percentage of the conductors during the coupling scheme and the achieved

Table 4. Capacity comparison of CS1 and CS2 module for different coupling schemes of type 2 (CS1 module: blue/CS2 module: red and the frequency spacing is equal to 0.1 MHz).

Power Grid Type	Coupling Schemes	Capacity (Mbps)				
		MV				
		Urban Case A	Urban Case B	Suburban Case	Rural Case	"LOS" case
Overhead	WtW^{1-2}	463/612	346/476	562/722	638/803	739/909
	WtW^{1-3}	465/615	348/478	565/725	639/804	741/911
	WtW^{1-4}	-	-	-	-	-
	WtW^{2-3}	463/612	346/476	562/722	638/803	739/909
	WtW^{2-4}	-	-	-	-	-
	WtW^{3-4}	-	-	-	-	-
Underground	PtP^{1-2}	698/815	581/685	767/890	838/968	913/1049
	PtP^{1-3}	698/815	581/685	767/890	838/968	913/1049
	PtP^{1-4}	-	-	-	-	-
	PtP^{2-3}	698/815	581/685	767/890	838/968	913/1049
	PtP^{2-4}	-	-	-	-	-
	PtP^{3-4}	-	-	-	-	-
		LV				
Overhead	WtW^{1-2}	463/612	346/475	562/721	637/803	738/908
	WtW^{1-3}	467/616	349/479	566/726	642/807	743/912
	WtW^{1-4}	466/615	348/478	566/725	641/806	742/911
	WtW^{2-3}	463/612	346/475	561/721	637/803	738/908
	WtW^{2-4}	464/613	347/477	536/723	639/804	740/909
	WtW^{3-4}	460/609	343/472	558/718	634/800	735/904
Underground	PtP^{1-2}	1634/1805	1420/1590	1739/1909	1838/2008	1938/2108
	PtP^{1-3}	1681/1851	1466/1636	1785/1955	1885/2055	1984/2154
	PtP^{1-4}	1635/1805	1420/1590	1739/1909	1838/2008	1937/2108
	PtP^{2-3}	1635/1805	1420/1590	1739/1909	1838/2008	1938/2108
	PtP^{2-4}	1681/1851	1466/1636	1785/1955	1885/2055	1984/2154
	PtP^{3-4}	1635/1805	1420/1590	1739/1909	1838/2008	1938/2108

capacity are analytically given.

Comparing Tables 3–5, it is evident that the coupling schemes of type 3 may present better capacity performance compared with the coupling schemes of type 1 and 2. In fact, the capacity increase may reach up to 74 Mbps. This capacity surplus may become crucial when BPL networks aim at providing reliable communications during an emergency (emergency BPL communications network). Nevertheless, it should be examined whether this capacity surplus of MtM coupling schemes is worth the installation of the additional pairs of BPL signal injectors and extractors across the existing BPL networks.

In addition, the capacity increase of MtM coupling schemes is achieved by mainly using the ground and the shield of overhead and underground distribution BPL networks, respectively, rather than differential excitations. This fact comes from the nonzero algebraic sum of the conductor participation percentage in the input coupling vector that implies a ground/shield return. But the use of either the ground or the shield excites the common mode across the MTL configurations. Notorious for its presence, common mode is responsible for increasing the EMI of BPL networks to the other communications services. Therefore, there is an interesting trade-off relation among capacity increase delivered by MtM coupling schemes, installation cost of additional BPL injectors/extractors and EMI.

Finally, coupling scheme type 3 is a simple theoretical expansion of the CS2 module of two conductors when three and four conductors are assumed without treating them as separate inputs and outputs like in MIMO systems. For the completeness of the theoretical analysis and comparison reasons, the coupling scheme type 3 has also been presented. Although coupling scheme type 3 acts as the theoretical best case scenario of CS2 module, its return on investment (ROI) is regarded as

Table 5. Top 5 coupling schemes of type 3 for distribution BPL LOS cases when CS2 module is applied (The frequency spacing is equal to 0.1 MHz and the participation percentage step is equal to 0.1).

Power Grid Type	Capacity (Mbps)			
	MV		LV	
	Coupling Schemes	"LOS" case	Coupling Schemes	"LOS" case
Overhead	$MtM^{1-2-3}_{0.8,-0.1,-0.1}$	921	$MtM^{1-2-3-4}_{0.7,-0.1,-0.1,-0.1}$	923
	$MtM^{1-2-3}_{-0.1,-0.1,0.8}$	921	$MtM^{1-3-4}_{0.8,-0.1,-0.1}$	921
	$MtM^{1-2-3}_{-0.2,-0.1,0.7}$	918	$MtM^{1-3-4}_{0.7,-0.2,-0.1}$	920
	$MtM^{1-2-3}_{-0.1,0.8,-0.1}$	918	$MtM^{1-2-3-4}_{0.6,-0.1,-0.1,-0.2}$	920
	$MtM^{1-2-3}_{0.7,-0.1,-0.2}$	918	$MtM^{1-2-3-4}_{0.6,-0.1,-0.2,-0.1}$	920
Underground	$MtM^{1-2}_{-0.9,-0.1}$	1049	$MtM^{1-2-4}_{-0.8,-0.1,-0.1}$	2228
	$MtM^{1-3}_{-0.9,-0.1}$	1049	$MtM^{1-2-3}_{-0.1,-0.8,-0.1}$	2228
	MtM^{1}_{-1}	1049	$MtM^{1-3-4}_{-0.1,-0.1,-0.8}$	2228
	$MtM^{1-3}_{-0.9,0.1}$	1049	$MtM^{1-2-3-4}_{-0.7,-0.1,0.1,-0.1}$	2203
	$MtM^{1-2}_{-0.9,0.1}$	1049	$MtM^{1-2-3-4}_{-0.1,-0.7,-0.1,0.1}$	2203

unacceptable in terms of the achieved capacity when MIMO and, more recently, massive MIMO can be deployed [41, 46, 47].

5.4. Discussion about CS2 Module and Its Supported Coupling Schemes

CS2 module can drastically change the coupling scheme stereotypes in distribution BPL networks, namely:

(1) By adopting CS2 module, WtW and PtP coupling schemes become almost equivalent to respective WtG and StP coupling schemes in terms of channel attenuation and capacity. In combination with their low EMI, coupling schemes of type 2 are going to be the leading coupling scheme type during the future's BPL network implementations.

(2) Since coupling schemes of low EMI will be deployed across the future's BPL networks, new EMI policies with higher IPSD limits concerning the BPL operation will be established and mandated. Furthermore, the synthesis of new higher IPSD limits and multiple input multiple output (MIMO) technology features may metamorphose BPL networks into a multi-Gbps backhaul network [41]. This multi-Gbps BPL network may support a myriad of smart grid applications including automated communication among components of the power grid, sensing, automated controls for repairs, energy trading and improved decision support software [42–45].

(3) Contrary to CS1 module, CS2 module supports the new coupling scheme type 3 that may involve all the conductors of the MTL configuration. Although coupling scheme type 3 achieves the best broadband performance metrics, there is a trade-off relation among the metric improvement, installation cost and EMI that needs further examination depending on the case scenario.

(4) Due to their tremendous capacity improvement, the deployment of MIMO schemes in distribution BPL networks, being well-known from the wireless world, is imperative in the following years. Hence, coupling schemes of type 3 may operate as the bridge between today's and future's BPL networks till appropriate EMI policies and network protocols are established.

6. CONCLUSIONS

This paper has focused on the broadband performance assessment of distribution BPL networks when CS2 module is considered. Based on its new BPL signal coupling procedure of two interfaces, CS2 module better exploits the existing conductors of the distribution MTL configurations as well as the injected and extracted power of BPL signals.

Synoptically, it has been shown that CS2 module maintains the same broadband performance of coupling schemes of type 1 compared with CS1 module. As it concerns the coupling schemes of type 2, CS2 module achieves to improve the channel attenuation and the capacity of distribution BPL networks on the basis of its advanced BPL signal extraction interface. In fact, the capacity increase may reach up to 170 Mbps when FCC Part 15 limits are considered in the 3–88 MHz frequency range. Compared with CS1 module, CS2 module introduces the coupling scheme type 3 that exploits all the available conductors of distribution MTL configurations. Although this type of coupling schemes may offer additional improvement of broadband performance metrics, there is a trade-off relation among the metric improvement, installation cost and EMI to other existing radioservices.

Finally, CS2 module renders coupling schemes of type 2 as the leading coupling trend. Due to their already known low-EMI features and the progress concerning their capacity, WtW and PtP coupling schemes are going to exclusively used during the design of the future's BPL networks.

REFERENCES

1. Lazaropoulos, A. G., "Towards modal integration of overhead and underground low-voltage and medium-voltage power line communication channels in the smart grid landscape: Model expansion, broadband signal transmission characteristics, and statistical performance metrics (invited paper)," *ISRN Signal Processing*, Vol. 2012, Article ID 121628, 1–17, 2012. [Online]. Available: http://www.hindawi.com/isrn/sp/2012/121628/.

2. Lazaropoulos, A. G., "Towards broadband over power lines systems integration: Transmission characteristics of underground low-voltage distribution power lines," *Progress In Electromagnetics Research B*, Vol. 39, 89–114, 2012.

3. Lazaropoulos, A. G. and P. G. Cottis, "Transmission characteristics of overhead medium voltage power line communication channels," *IEEE Trans. Power Del.*, Vol. 24, No. 3, 1164–1173, Jul. 2009.

4. Lazaropoulos, A. G. and P. G. Cottis, "Capacity of overhead medium voltage power line communication channels," *IEEE Trans. Power Del.*, Vol. 25, No. 2, 723–733, Apr. 2010.

5. Lazaropoulos, A. G. and P. G. Cottis, "Broadband transmission via underground medium-voltage power lines — Part I: Transmission characteristics," *IEEE Trans. Power Del.*, Vol. 25, No. 4, 2414–2424, Oct. 2010.

6. Lazaropoulos, A. G. and P. G. Cottis, "Broadband transmission via underground medium-voltage power lines — Part II: Capacity," *IEEE Trans. Power Del.*, Vol. 25, No. 4, 2425–2434, Oct. 2010.

7. Lazaropoulos, A. G., "Broadband transmission characteristics of overhead high-voltage power line communication channels," *Progress In Electromagnetics Research B*, Vol. 36, 373–398, 2012.

8. Lazaropoulos, A. G., "Green overhead and underground multiple-input multiple-output medium voltage broadband over power lines networks: Energy-efficient power control," *Springer Journal of Global Optimization*, Vol. 2012, 1–28, Oct. 2012, Print ISSN 0925-5001.

9. Ferreira, H., L. Lampe, J. Newbury, and T. G. Swart, *Power Line Communications, Theory and Applications for Narrowband and Broadband Communications over Power Lines*, Wiley, New York, 2010.

10. Lazaropoulos, A. G., "Deployment concepts for overhead high voltage broadband over power lines connections with two-hop repeater system: Capacity countermeasures against aggravated topologies and high noise environments," *Progress In Electromagnetics Research B*, Vol. 44, 283–307, 2012.

11. Lazaropoulos, A. G., "Broadband transmission and statistical performance properties of overhead high-voltage transmission networks," *Hindawi Journal of Computer Networks and Commun.*, article ID 875632, 2012. [Online]. Available: http://www.hindawi.com/journals/jcnc/aip/875632/

12. Amirshahi, P. and M. Kavehrad, "High-frequency characteristics of overhead multiconductor power lines for broadband communications," *IEEE J. Sel. Areas Commun.*, Vol. 24, No. 7, 1292–1303, Jul. 2006.

13. Calliacoudas, T. and F. Issa, ""Multiconductor transmission lines and cables solver", An efficient simulation tool for PLC channel networks development," *IEEE Int. Conf. Power Line Communications and Its Applications*, Athens, Greece, Mar. 2002.

14. Sartenaer, T. and P. Delogne, "Deterministic modelling of the (Shielded) outdoor powerline channel based on the multiconductor transmission line equations," *IEEE J. Sel. Areas Commun.*, Vol. 24, No. 7, 1277–1291, Jul. 2006.

15. Paul, C. R., *Analysis of Multiconductor Transmission Lines*, Wiley, New York, 1994.

16. Meng, H., S. Chen, Y. L. Guan, C. L. Law, P. L. So, E. Gunawan, and T. T. Lie, "Modeling of transfer characteristics for the broadband power line communication channel," *IEEE Trans. Power Del.*, Vol. 19, No. 3, 1057–1064, Jul. 2004.

17. Li, B., D. Mansson, and G. Yang, "An efficient method for solving frequency responses of power-line networks," *Progress In Electromagnetics Research B*, Vol. 62, 303–317, 2015.

18. Chaaban, M., K. El Khamlichi Drissi, and D. Poljak, "Analytical model for electromagnetic radiation by bare-wire structures," *Progress In Electromagnetics Research B*, Vol. 45, 395–413, 2012.

19. Kim, Y. H., S. Choi, S. C. Kim, and J. H. Lee, "Capacity of OFDM two-hop relaying systems for medium-voltage power-line access networks," *IEEE Trans. Power Del.*, Vol. 27, No. 2, 886–894, Apr. 2012.

20. Amirshahi, P. and M. Kavehrad, "Medium voltage overhead powerline broadband communications; Transmission capacity and electromagnetic interference," *Proc. IEEE Int. Symp. Power Line Commun. Appl.*, 2–6, Vancouver, BC, Canada, Apr. 2005.

21. OPERA1, D44: Report presenting the architecture of plc system, the electricity network topologies, the operating modes and the equipment over which PLC access system will be installed, IST Integr. Project No 507667, Dec. 2005.

22. OPERA1, D5: Pathloss as a function of frequency, distance and network topology for various LV and MV European powerline networks. IST Integrated Project No 507667, Apr. 2005.

23. Veen, J., P. C. J. M. van der Wielen, and E. F. Steennis, "Propagation characteristics of three-phase belted paper cable for on-line PD detection," *Proc. 2002 IEEE International Symposium on Electrical Insulation, ELINSL02*, 96–99, Boston, MA, USA, Apr. 2002.

24. Van der Wielen, P. C. J. M., E. F. Steennis, and P. A. A. F. Wouters, "Fundamental aspects of excitation and propagation of on-line partial discharge signals in three-phase medium voltage cable systems," *IEEE Trans. Dielectr. Electr. Insul.*, Vol. 10, No. 4, 678–688, Aug. 2003.

25. Tang, M. and M. Zhai, "Research of transmission parameters of four-conductor cables for power line communication," *Proc. Int. Conf. on Computer Science and Software Engineering*, Vol. 5, 1306–1309, Wuhan, China, Dec. 2008.

26. Issa, F., D. Chaffanjon, E. P. de la Bathie, and A. Pacaud, "An efficient tool for modal analysis transmission lines for PLC networks development," *IEEE Int. Conf. Power Line Communications and Its Applications*, Athens, Greece, Mar. 2002.

27. D'Amore, M. and M. S. Sarto, "A new formulation of lossy ground return parameters for transient analysis of multiconductor dissipative lines," *IEEE Trans. Power Del.*, Vol. 12, No. 1, 303–314, Jan. 1997.

28. D'Amore, M. and M. S. Sarto, "Simulation models of a dissipative transmission line above a lossy ground for a wide-frequency range — Part I: Single conductor configuration," *IEEE Trans. Electromagn. Compat.*, Vol. 38, No. 2, 127–138, May 1996.

29. D'Amore, M. and M. S. Sarto, "Simulation models of a dissipative transmission line above a lossy ground for a wide-frequency range — Part II: Multi-conductor configuration," *IEEE Trans. Electromagn. Compat.*, Vol. 38, No. 2, 139–149, May 1996.

30. Anatory, J., N. Theethayi, R. Thottappillil, M. M. Kissaka, and N. H. Mvungi, "The influence of load impedance, line length, and branches on underground cable power-line communications (PLC) systems," *IEEE Trans. Power Del.*, Vol. 23, No. 1, 180–187, Jan. 2008.

31. Lazaropoulos, A. G., "Factors influencing broadband transmission characteristics of underground low-voltage distribution networks," *IET Commun.*, Vol. 6, No. 17, 2886–2893, Nov. 2012.

32. Anatory, J., N. Theethayi, and R. Thottappillil, "Power-line communication channel model for interconnected networks — Part II: Multiconductor system," *IEEE Trans. Power Del.*, Vol. 24, No. 1, 124–128, Jan. 2009.

33. Anatory, J., N. Theethayi, R. Thottappillil, M. M. Kissaka, and N. H. Mvungi, "The effects of load impedance, line length, and branches in typical low-voltage channels of the BPLC systems of developing countries: Transmission-line analyses," *IEEE Trans. Power Del.*, Vol. 24, No. 2, 621–629, Apr. 2009.

34. Gebhardt, M., F. Weinmann, and K. Dostert, "Physical and regulatory constraints for communication over the power supply grid," *IEEE Commun. Mag.*, Vol. 41, No. 5, 84–90, May 2003.

35. Henry, P. S., "Interference characteristics of broadband power line communication systems using aerial medium voltage wires," *IEEE Commun. Mag.*, Vol. 43, No. 4, 92–98, Apr. 2005.

36. Ofcom, "Amperion PLT Measurements in Crieff," Ofcom, Tech. Rep., Sept. 2005.

37. NATO, "HF Interference, Procedures and Tools (Interferences HF, procedures et outils) Final Report of NATO RTO Information Systems Technology," RTO-TR-ISTR-050, Jun. 2007, [Online]. Available: http://ftp.rta.nato.int/public/PubFullText/RTO/TR/RTO-TR-IST-050/TR-IST-050-ALL.pdf

38. FCC, "In the Matter of Amendment of Part 15 regarding new requirements and measurement guidelines for Access Broadband over Power Line Systems," FCC 04-245 Report and Order, Jul. 2008.

39. Ofcom, "DS2 PLT Measurements in Crieff," Ofcom, Tech. Rep. 793 (Part 2), May 2005.

40. Ofcom, "Ascom PLT Measurements in Winchester," Ofcom, Tech. Rep. 793 (Part 1), May 2005.

41. Lazaropoulos, A. G., "Broadband over Power Lines (BPL) systems convergence: Multiple-Input Multiple-Output (MIMO) communications analysis of overhead and underground low-voltage and medium-voltage BPL networks (invited paper)," *ISRN Power Engineering*, Vol. 2013, Article ID 517940, 1–30, 2013. [Online]. Available: http://www.hindawi.com/isrn/power.engineering/2013/517940/.

42. El Haj, Y., L. Albasha, A. El-Hag, and H. Mir, "Data communication through distribution networks for smart grid applications," *IET Science, Measurement & Technology*, Vol. 9, No. 6, 774–781, 2015.

43. Lazaropoulos, A. G., "Wireless sensor network design for transmission line monitoring, metering and controlling: Introducing Broadband over PowerLines-enhanced Network Model (BPLeNM)," *ISRN Power Engineering*, Vol. 2014, Article ID 894628, 22 pages, 2014, doi:10.1155/2014/894628. [Online]. Available: http://www.hindawi.com/journals/isrn.power.engineering/2014/894628/.

44. Lazaropoulos, A. G., "Wireless sensors and broadband over powerlines networks: The performance of Broadband over PowerLines-enhanced Network Model (BPLeNM) (invited paper)," *ICAS Publishing Group Transaction on IoT and Cloud Computing*, Vol. 2, No. 3, 1–35, 2014. [Online]. Available: http://icas-pub.org/ojs/index.php/ticc/article/view/27/17.

45. Lazaropoulos, A. G. and P. Lazaropoulos, "Financially stimulating local economies by exploiting communities' microgrids: Power trading and Hybrid Techno-Economic (HTE) model," *Trends in Renewable Energy*, Vol. 1, No. 3, 131–184, Sept. 2015. [Online]. Available: http://futureenergysp.com/index.php/tre/article/view/14.

46. Lazaropoulos, A. G., "Overhead and underground MIMO low voltage broadband over power lines networks and EMI regulations: Towards greener capacity performances," *Elsevier Computers and Electrical Engineering*, Vol. 39, 2214–2230, 2013.

47. Lazaropoulos, A. G., "Policies for carbon energy footprint reduction of overhead multiple-input multiple-output high voltage broadband over power lines networks," *Trends in Renewable Energy*, Vol. 1, No. 2, 87–118, Jun. 2015. [Online]. Available: http://futureenergysp.com/index.php/tre/article/view/11/17.